Front. Optoelectron. 2012, 5(4): 457–464
DOI 10.1007/s12200-012-0289-3

RESEARCH ARTICLE

Proposal for modeling of tapered quantum-dot semiconductor optical amplifiers

Ehsan MOHADESRAD, Kambiz ABEDI (✉)

Department of Electrical Engineering, Faculty of Electrical and Computer Engineering, Shahid Beheshti University, Tehran 1983963113, Iran

Abstract To compensate for the loss of carrier density along the active region of quantum-dot semiconductor optical amplifiers (QD-SOAs), tapered structure of the waveguide is introduced. In this paper, a method for theoretically modeling of such devices is proposed, and according to that model different shapes of tapered waveguides are studied. This study is pivoted around the optical gain and cross-gain modulation (XGM) of the QD-SOA under investigation to show how altering the shape of the waveguide affects the main characteristics of the device. For doing so, the rate equation model has been employed and solved through finite difference method and MATLAB ODE. Through this, as long as monotonically increasing profiles for the width of the waveguide are used, the shape of the waveguide has a negligible effect on the gain which mainly depends on the width ratio of the waveguide output to its input. However, this carrier compensation has adverse effect on the XGM, where its efficiency rely on how the pump signal can effectively reduce carrier density and upset the gain.

Keywords tapered waveguide, cross-gain modulation (XGM), quantum-dot (QD), semiconductor optical amplifier (SOA)

1 Introduction

Quantum-dot semiconductor optical amplifiers (QD-SOAs) in comparison with bulk and quantum-well SOAs (QW-SOAs) have shown improvements in their output power, threshold current, temperature stability, noise characteristics and presented interesting nonlinear properties. These and other merits of QD-SOAs bring about good opportunities in utilizing them as building blocks of all-optical systems [1–4]. However, in QD-SOAs as well as SOAs because of the carrier density reduction in the direction of signal propagation along the waveguide, gain is regionally different and diminishing. In other words, as a result of increasing stimulated emission due to the optical signal amplification along the active region, optical gain of the QD-SOA is nonlinearly decreasing [5–7].

Theoretically to compensate carrier density in the far side of the QD-SOA, a nonlinear profile of injected current can be applied where this profile dictates a nonuniform increasing current [8]. Practically nonuniform current injection could be realized through multielectrode QD-SOAs [9]. In such devices, different currents will be conducted via two or more electrodes into the waveguide in a manner, in which higher currents will reach to farther regions of the QD-SOA where the carrier density is more compromised [10]. To avoid complicated driving circuits, especially for more than two electrodes and other difficulties which arise with implementing several electrodes, tapered waveguide approach can be employed. In this method, increasing width of the waveguide provides more QDs for our optical signal as the signal travels through the QD-SOA and so optical gain compensating along the active region can be achieved.

To this end, we first introduce our QD-SOA model and its rate equations, then a method for modeling tapered waveguide structure for QD-SOAs is proposed. In the end, we proceed with examining gain and cross-gain modulation (XGM) of the device in this new structure.

2 Physical structure and theory of typical QD-SOA

The device under investigation is an InAs/GaAs QD-SOA and as it depicted in Fig. 1, seven stacked layers of self-assembled InAs QDs on a GaAs substrate formed the active region of this QD-SOA. The density of QDs in every one of these layers is 5.0×10^{10} cm^{-2} and each have a 5 nm

Received September 5, 2012; accepted October 12, 2012

E-mail: K_Abedi@sbu.ac.ir

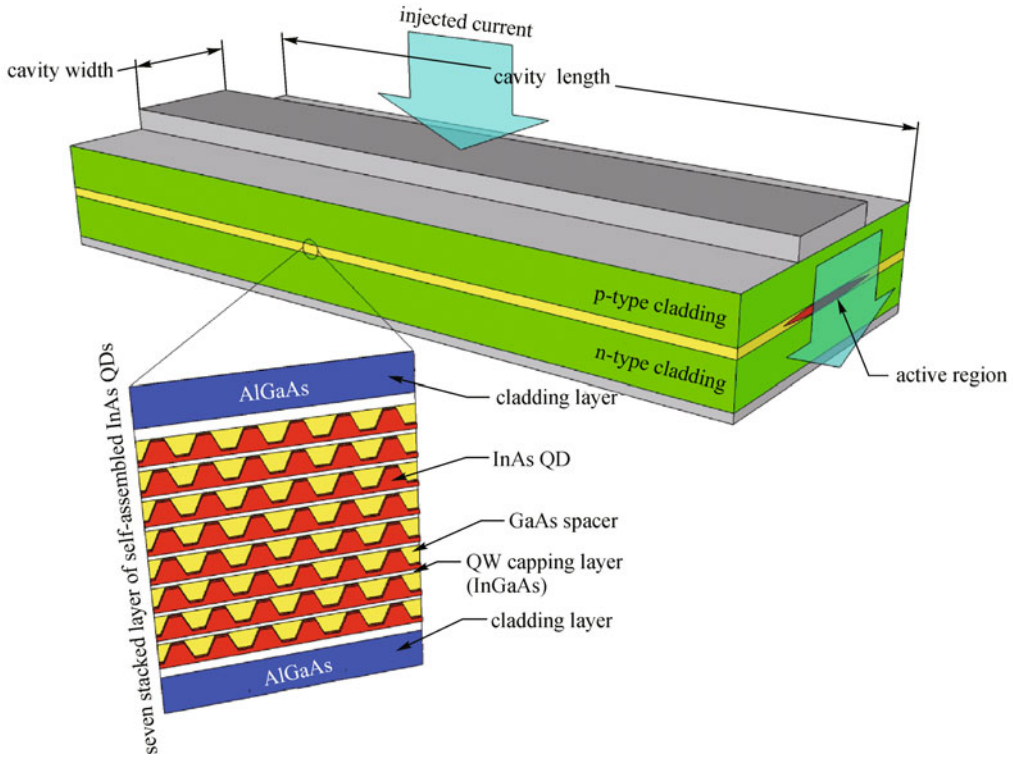

Fig. 1 Schematic diagram of QD-SOA

thick InGaAs capping layer. For strain relaxation between adjoining layers, a 33 nm thick GaAs isolating layer is implemented [8].

Figure 2 shows the energy band diagram of this QD-SOA, where its conduction and valence bands (CB and VB) have three and eight non-degenerate energy levels respectively. Also each band has an energy level usually called wetting layer (WL), which act as a reservoir for the other levels within the band (excited states (ESs) and ground state (GS)).

We employed rate equation model to describe changes in occupation probabilities as the optical signal travels through active region and being amplified due to the stimulated emission. Moreover, these equations take into account injection current from outside replenishing carrier reservoirs, and the terms have been referred to WL and subsequently ESs.

In this model of rate equations, which is known as "electron-hole model", the dynamics of the electron and hole were dealt with separately [11]. The specific version of the rate equations that has been used in this study is described as follows.

The electrons rate equation in the conduction band's GS is [12]:

$$\frac{\partial f_0^n}{\partial t} = (R_{1,0}^{nc} - R_{0,1}^{ne}) - R_0^{sp} - R_0^{st}, \quad (1)$$

and for the i th ES of CB, the rate equation is given by

$$\frac{\partial f_i^n}{\partial t} = (R_{i+1,i}^{nc} - R_{i,i+1}^{ne}) - (R_{i,i-1}^{nc} - R_{i-1,i}^{ne}) - R_i^{sp} - R_i^{st}, \quad (2)$$

where f_i is the occupation probability in i th state. $R_{i+1,i}^{nc} = R_{i+1,i}^{nc}(z,t)$ and $R_{i,i+1}^{ne} = R_{i,i+1}^{ne}(z,t)$ represent electron capture rate from $(i+1)$ th state to i th state and electron escape rate from the i th state to $(i+1)$ th state, respectively. Spontaneous emission rate and stimulated emission rate of the i th state are taken into account by R_i^{sp} and R_i^{st}, which are given by [12]

$$R_i^{sp} = \frac{f_i^n f_i^p}{\tau_{iR}}(a_{ii}^n + c_{ii}^p f_i^p + c_{ii}^n f_i^n), \quad (3)$$

$$R_i^{st} = \frac{\upsilon_g g_i}{N_Q}(f_i^p + f_i^n - 1)S, \quad (4)$$

in which τ_{iR} is the spontaneous radiative lifetime in i th state, a_{ii}^n is the phonon-assisted coefficient and N_Q is the density of QDs per unit volume. S and g, which are the photon density and the gain dispersion, will be defined later.

c_{ii}^n and c_{ii}^p are introduced as Auger-assisted coefficients [7,12] to take into account the effect of doping, which can lead to a notable increase in non-radiative recombination processes, such as Auger recombination (especially when injected current is increasing) [13].

The rate equation for CB's WL is given by [12]

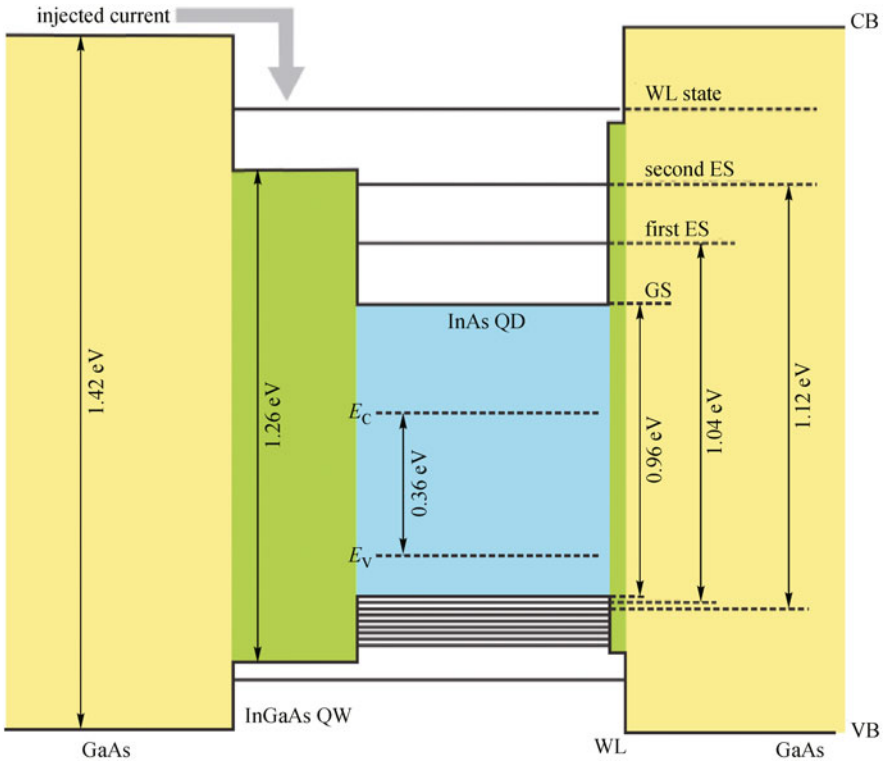

Fig. 2 Energy band diagram of one layer of QDs schematically depicting energy gaps between CB and VB states [8]

$$\frac{\partial w_n}{\partial t} = \frac{I}{qV_aN_{WL}} - (R^{nc}_{w_n,2} - R^{ne}_{2,w_n}) - R^{sp}_{w_n} + D_n\frac{\partial^2 w_n}{\partial z^2}, \quad (5)$$

where q is the electron charge, V_a is the volume of the WL, and N_{WL} is the maximum carrier density at the WL. I is the injected current and D_n is the electron diffusion coefficient [9]. In this paper, each QD is studied as an independent entity from other QDs, and as a result of this assumption, the carrier diffusion between QDs is ignored.

Since there are eight states in the VB and the equations for the first three hole states are exactly the same as electron states in the CB, therefore the rate equation for other five hole states are given as [12]

$$\frac{\partial f^p_k}{\partial t} = (R^{pc}_{k+1,k} - R^{pe}_{k,k+1}) - (R^{pc}_{k,k-1} - R^{pe}_{k-1,k}), \quad (6)$$

where $k(k \geqslant 3)$, denotes the hole energy state number. $R^{pc}_{k+1,k} = R^{pc}_{k+1,k}(z,t)$ and $R^{pe}_{k,k+1} = R^{pe}_{k,k+1}(z,t)$ represent holes capture rate from $(k+1)$ th state to the k th state and holes escape rate from the k th state to $(k+1)$ th state, respectively.

The carrier rate equation for valance band's WL is not so different from CB's WL and is given by [12]

$$\frac{\partial w_p}{\partial t} = \frac{I}{qV_aN_{WL}} - (R^{nc}_{wp,7} - R^{ne}_{7,wp}) - R^{sp}_{wp} + D_p\frac{\partial^2 w_p}{\partial z^2}, \quad (7)$$

where D_p is the valance band's WL diffusion coefficient [9].

The rate equation of the photon density of the optical signal propagating through active region is [12]

$$\frac{\partial S}{\partial z} = g_{\mathrm{QD}}S - \alpha S, \quad (8)$$

where α, which is assumed to be wavelength independence, is denoting the waveguide loss. S is the propagating photon density and g_{QD} is the modal gain, where both of them are functions of time and position, g_{QD} is given by [12,14]

$$g_{\mathrm{QD}} = \sum_{j=0}^{H} g_j\left(f^n_j + f^p_j - 1\right), \quad (9)$$

where the upper limit of the series, H, is the number of transitions which is the same as the number of CB states and g_j is the gain dispersion for the j th transition given by [12]

$$g_j = g^{\max}_j \frac{\hbar\omega^{\max}_j}{\hbar\omega}\exp\left(\frac{-(\hbar\omega - \hbar\omega^{\max}_j)^2}{2\sigma^2_j}\right), \quad (10)$$

where $g^{\max}_j$ is the maximum gain coefficient for the j th transition, σ_j is the inhomogeneous line broadening, $\hbar\omega$ is the photon energy of the input signal, and $\hbar\omega^{\max}_j$ is the

energy where the gain for the j th transition is maximum.

Physical parameters of the QD-SOA under investigation regarding to the following simulations are presented in Table 1 [8].

Table 1 Physical parameters of QD-SOA under investigation [8]

symbol	value	symbol	value
L	3 mm	τ_{0R}	0.2 ns
W	4 μm	τ_{1R}	0.2 ns
L_w	0.2 μm	τ_{wR}	0.2 ns
H	2	$\tau^n_{1,0}$	8 ps
$\hbar\omega_0^{\max}$	0.962 eV	$\tau^n_{2,1}$	2 ps
$\hbar\omega_1^{\max}$	1.042 eV	$\tau^n_{3,2}$	0.8 ps
$\hbar\omega_2^{\max}$	1.122 eV	$\tau^n_{0,1}$	80 ps
$g_0^{\max}$	14 cm^{-1}	$\tau^n_{1,2}$	20 ps
$g_1^{\max}$	20 cm^{-1}	$\tau^n_{2,3}$	8 ps
$g_2^{\max}$	~0 cm^{-1}	$\tau^p_{k+1,k}$	0.5 ps
α	4 cm^{-1}	$\tau^p_{k,k+1}$	0.74 ps
σ_j	30 meV	$a^{n,p}_{ji}$	1
q	1.602×10^{-19} C	$a^{n,p}_{ii}$	1
v_g	8.45×10^9 $cm \cdot s^{-1}$	c^p_{ii}	0.2
N_Q	2.5×10^{17} cm^{-3}	$c^{nn}_{1,0}$	27
N_{WL}	5.4×10^{17} cm^{-3}	$c^{np}_{1,0}$	175
D_n	879 $cm^2 \cdot s^{-1}$	$c^{nn}_{2,1}$	7
D_P	13.7 $cm^2 \cdot s^{-1}$	$c^{np}_{1,0}$	35

Note that these rate equations are time differential equations, so in order to study carrier density variations in QD-SOA along the direction of propagating signal, we assumed that the device under investigation are assembled of many extremely short serialized QD-SOAs which in every one of them local carrier density and photon density variations is negligible (Fig. 3). We have utilized Matlab ODE to solve this set of rate equations for one slice of the QD-SOA and calculated the photon density and the carrier density for all time frames in regard to that slice, and then by employing FDM, we have used those results to generate required boundary conditions for the next slice, and so on to the end of the QD-SOA.

3 Tapered waveguide structure and modeling

The problem with conventional straight waveguide structures, Fig. 4(a), is that the carrier density, which is the main factor in optical amplification, reduces as the light intensity increases along the active region. This reduction in carrier density actively contributes in pressing gain saturation boundary, which greatly limits the application of the QD-SOA [2]. Increasing the width of active region to provide more carriers in order to avoid gain saturation can also results in multiple transverse mode propagation [6]. To overcome this problem and yet provide the carriers needed, Ref. [15] has proposed employing the method in which the width of the waveguide gradually increases as light travels from the input to the output of the amplifier. This tapered structure, which is depicted in Fig. 4(b), allows most of the optical power still remains in fundamental mode and delivers a gain with high saturation power as well.

In this section, first our model of tapered structure is introduced to promote the solution, with which we have modified the equations to accept increasing width of the waveguide. Then, various types of tapered structure to find the optimum model for our goal are studied.

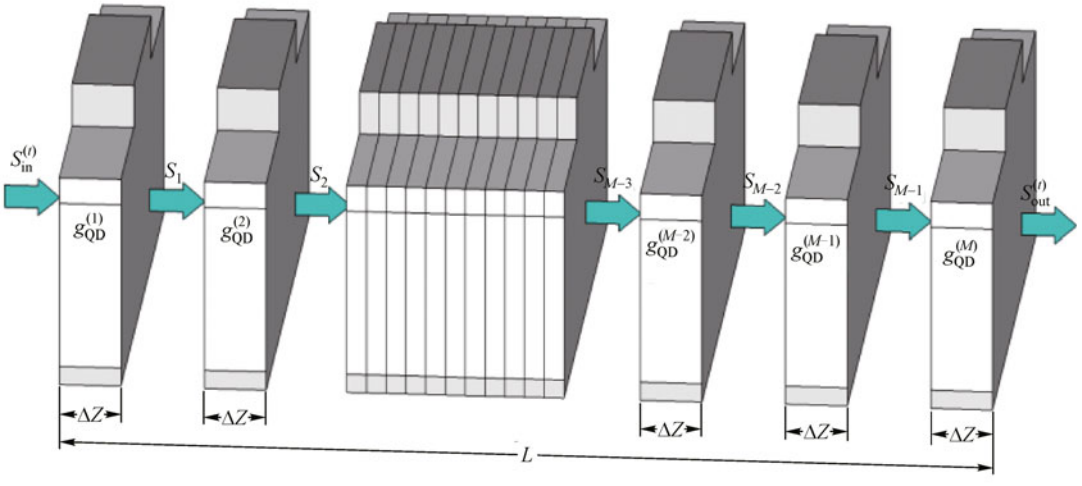

Fig. 3 Schematic of QD-SOA, comprised of extremely short sections

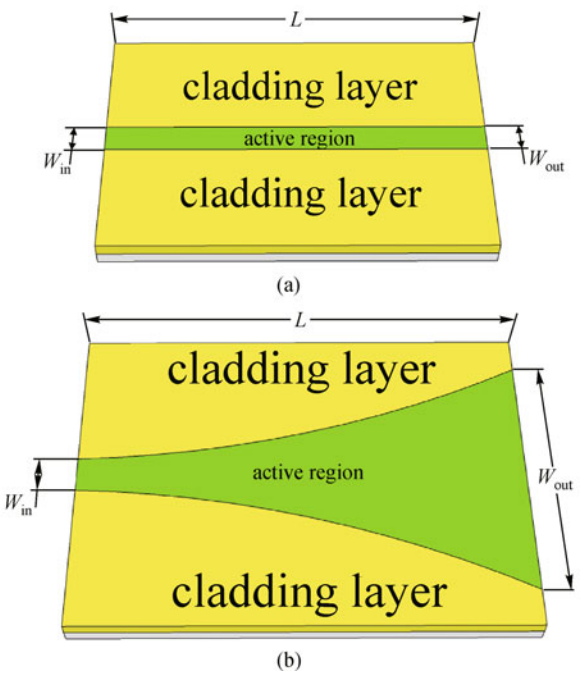

Fig. 4 (a) Conventional straight waveguide structure; (b) tapered waveguide structure

To introduce a practical model, two conditions for the tapered structures were assumed, where these conditions in every type of them were considered to be true [6]. These two conditions are uniformity and instantaneity in the propagation of optical power and intensity in the plane of the cross-section of the waveguide as signal travels through amplifier and experiences widening of the waveguide. This allows us to suppose that lateral optical intensity is no longer a function of lateral position, therefore optical intensity has a constant value across the waveguide in a specific time frame.

To simplify our understanding of the tapered structure, Fig. 5(a) is illustrated. As you can see, with increase in the width of the waveguide, the optical intensity reduces; this reduction in optical intensity is reverse proportional to the width. But if we want to model the tapered structure as already well-known conventional QD-SOA with straight cavity, we may presume, as depicted in Fig. 5(b) that instead of widening of the waveguide, the QDs density increases along the waveguide and this increase is proportional to the width. So in our tapered structure modeling, we can assume that the QD-SOA has a conventional straight cavity but we should impose extra reduction on the optical intensity as signal travels through waveguide, and this infliction must be reverse proportional to the width; or we can simply assume that the QD density is increasing in proportion to the width. As you can see in Eq. (11), which describes the stimulated emission rate, these two approaches (photon density reduction and QD density increment) have exactly the same effect on the stimulated emission.

$$R_i^{st} = \frac{v_g g_i}{N_Q}(f_i^p + f_i^n - 1)S. \tag{11}$$

According to the premise established, Eq. (11) can be modified to Eq. (12), where $W(z)$ is the width of the waveguide at z.

$$R_i^{st} = \frac{v_g g_i}{N_Q}(f_i^p + f_i^n - 1)S \times \left(\frac{W_{\text{in}}}{W(z)}\right). \tag{12}$$

If extra reduction on the photon density is imposed as the width increases, in the end of procedure when photon-density at the output of the QD-SOA is measured, we may

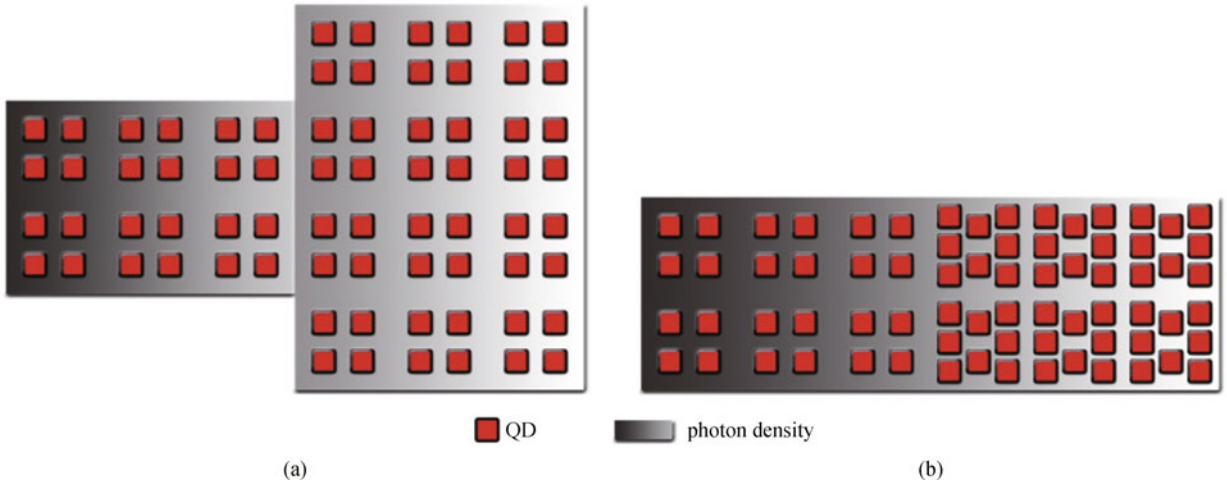

Fig. 5 (a) Exaggerated tapered structure; (b) tapered structure modeled as conventional QD-SOA with increasing QD density

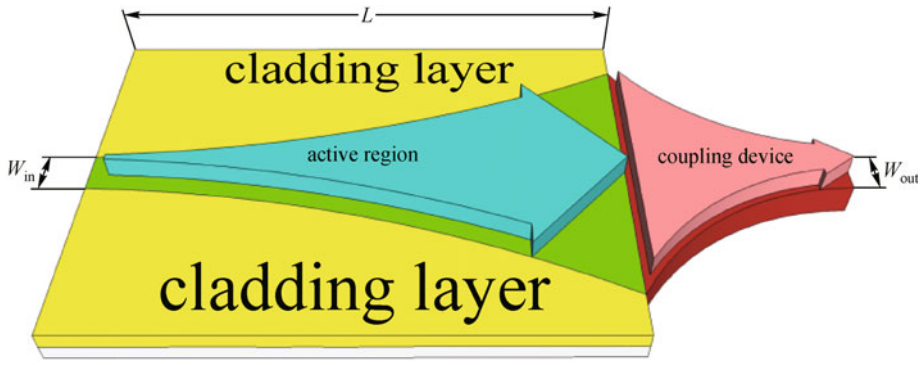

Fig. 6 Schematic diagram of QD-SOA with coupling device to back to initial width

face with smaller photon density than conventional structure, but because of the increase in the output facet area due to the tapered structure, we will have much more photons [6]. If we imagine that we have a coupling structure at the end of the device with the output width of the QD-SOA's input, we may multiply the photon-density by QD-SOA's W_{out}/W_{in}. This notion is depicted in Fig. 6.

4 Gain and XGM results for tapered structure

For this study, we employed a train of "1" optical pulses, where the pulses were considered to be Gaussian with the pulse width of 0.4 ps. To be sure that optical pulses will lead the QD-SOA to gain saturation, the pulses' energy is assumed to be 200 fj, equivalent to the signal with average power of 100 mW at 500 Gbits/s. Normalized constant injected current which is also defined in Ref. [8], was assumed to be 4.

The types of tapered structures have been studied in order to find optimum types are presented in Table 2. Optical gain and XGM have been considered to be the targets of the study. To hold to the conditions stated before (uniformity and instantaneity), the ratio of output width to input width has been limited to the maximum of 20:1.

Figure 7 shows the effect of increasing the width ratio of an exponential tapered structure on the modal gain. This gain obtained at the end of the device which was expected to be depleted of carriers and as you can see, the compensation through widening the waveguide has a satisfactory effect on the gain. As the width ratio increases, the gain line approaches its maximum level and also the changes in the gain are growing smaller with each increment, in a way that the width ratio above 10 has a small effect, so maybe it is a fair choice. Output signals photon densities during simulation period for different width ratios are illustrated in Fig. 8.

Table 2 Shapes of tapered wave-guide

shapes	equation	parameters
square root	$J(z)=\sqrt{az+b^2}$	a,b
quadratic	$J(z)=az^2+b$	a,b
linear	$J(z)=az+b$	a,b
exponential	$J(z)=b\exp(az)$	a,b

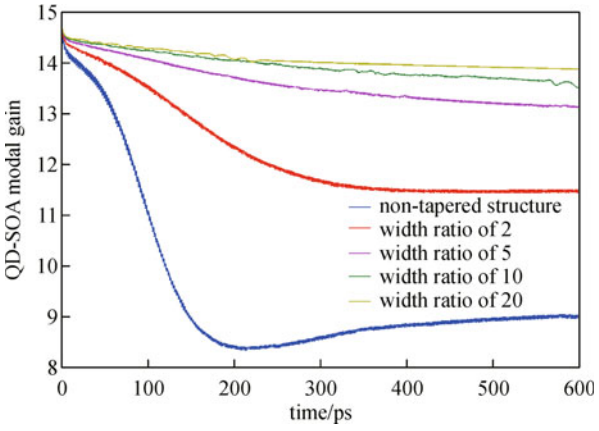

Fig. 7 Tapered QD-SOA modal gain for different width ratios at the end of device

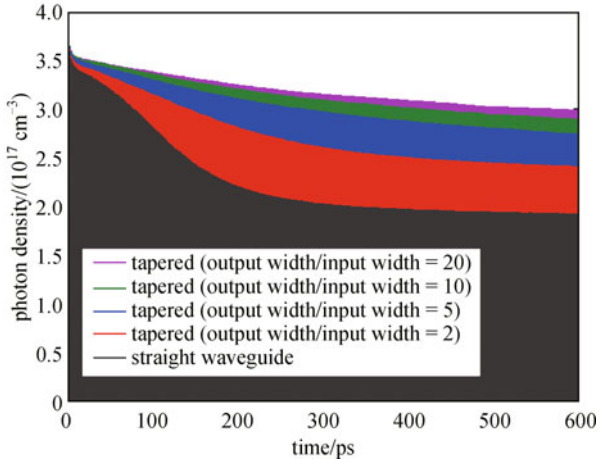

Fig. 8 Tapered QD-SOA output signals photon densities for different width ratios at the end of device

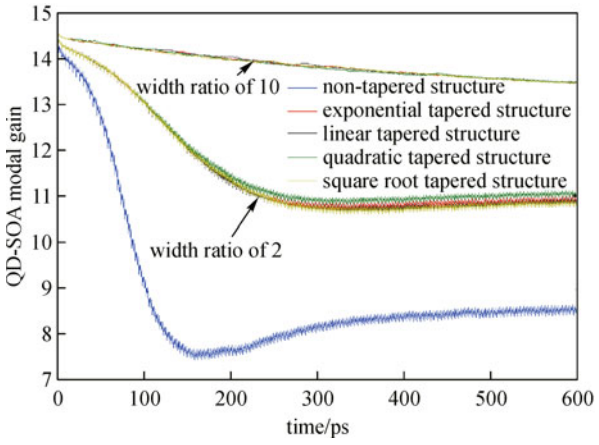

Fig. 9 Tapered QD-SOA modal gain for different shapes of waveguide with width ratio of 2 and 10 at the end of device

The results for different shapes of tapered structure are demonstrated in Fig. 9 and show that the types have been used according to Table 2 where all are continuously increasing functions, and all reach the same width at the end, follow almost same pattern of gain, and as the width ratio increases, these patterns become more indistinguishable. As been discussed earlier, these results can be multiplied by the width ratio, provided a coupling device that has been used to back to the initial width.

To study the XGM response of tapered QD-SOA, we employed the probe signal of 0.1 mW light power, at 1193 nm, and the pump signal of 10 mW average light power, at 1289 nm. The pump signal amplitude is 10 mW (half of the peak-to-peak power). The XGM results for tapered structure are depicted in Fig. 10. These results make evident if we donot want to lose the XGM efficiency dramatically and also secure a decent gain for our tapered QD-SOA, we may limit our width ratio to 2. This drop in the XGM efficiency can be explained with a reservoir analogy. Increasing the width of the waveguide is similar to increasing gradually the volume of a reservoir. By doing so, it is beginning to get harder to emptying and replenishing this reservoir, so the pump signal cannot accomplish its goal to affect the gain of the QD-SOA by draining it of the carriers. So the probe signal leaves the QD-SOA less affected.

5 Conclusions

In this paper, a model for tapered waveguide structure of QD-SOA was proposed. Through this method, several shapes of waveguides along different width ratios has been studied. We demonstrated that as long as width of the waveguide has a monotonically increasing profile, the shape of the waveguide has a small effect on the gain. It has been shown that increasing width ratio of the waveguide could definitely enhance the gain; however with each step up in width ratio, this enhancement became lesser. In the case of the XGM, we observed that for too widened tapered structure, the XGM efficiency dropped significantly which was related to the pump signal incapable of altering the gain substantially. One may conclude that we can preserve the XGM along with a decent gain should we limit the width ratio to 2.

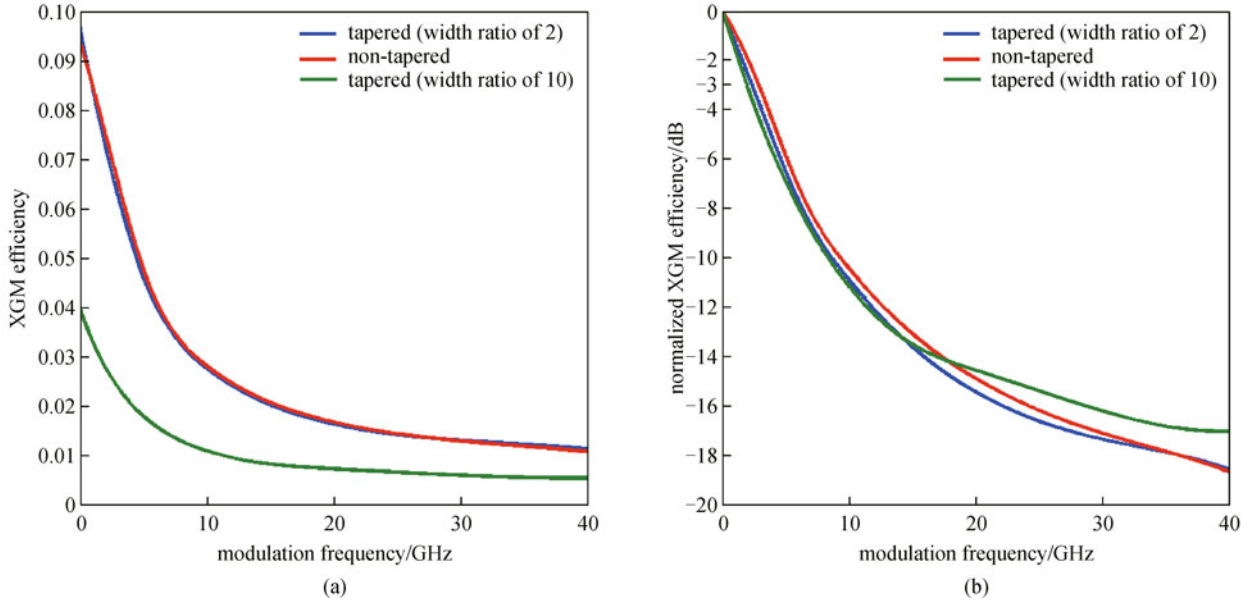

Fig. 10 XGM efficiency (a) and normalized XGM efficiency (b)

References

1. Rostami A, Baghban H, Maram R. Nanostructure Semiconductor Optical Amplifiers: Building Blocks for All-Optical Processing. New York: Springer Heidelberg, 2011
2. Akiyama T, Sugawara M, Arakawa Y. Quantum-dot semiconductor optical amplifiers. Proceedings of the IEEE, 2007, 95(9): 1757–1766
3. Bilenca A, Eisenstein G. On the noise properties of linear and nonlinear quantum-dot semiconductor optical amplifiers: the impact of inhomogeneously broadened gain and fast carrier dynamics. IEEE Journal of Quantum Electronics, 2004, 40(6): 690–702
4. Akiyama T, Hatori N, Nakata Y, Ebe H, Sugawara M. Pattern-effect-free semiconductor optical amplifier achieved using quantum dots. Electronics Letters, 2002, 38(19): 1139–1140
5. Connelly M J. Semiconductor Optical Amplifiers. Boston: Kluwer Academic Publishers, 2002
6. Ghafouri-Shiraz H. The Principles of Semiconductor Laser Diodes and Amplifiers: Analysis and Transmission Line Laser Modeling. London: Imperial College Press, 2004
7. Qasaimeh O. Effect of doping on the optical characteristics of quantum-dot semiconductor optical amplifiers. Lightwave Technology Journalism, 2009, 27(12): 1978–1984
8. Taleb H, Abedi K, Golmohammadi S. Operation of quantum-dot semiconductor optical amplifiers under nonuniform current injection. Applied Optics, 2011, 50(5): 608–617
9. Yi Y, Lirong H, Meng X, Peng T, Dexiu H. Enhancement of gain recovery rate and cross-gain modulation bandwidth using a two-electrode quantum-dot semiconductor optical amplifier. Journal of the Optical Society of America B, Optical Physics, 2010, 27(11): 2211–2217
10. Carney K, Latkowski S, Maldonado-Basilio R, Landais P, Lennox R, Bradley A L. Characterization of a multi-electrode bulk-SOA for low NF in-line amplification in passive optical networks. In: Proceedings of the 12th International Conference on Transparent Optical Networks (ICTON), 2010, 1–4
11. Fiore A, Markus A. Differential gain and gain compression in quantum-dot lasers. IEEE Journal of Quantum Electronics, 2007, 43 (4): 287–294
12. Qasaimeh O R. Ultra-fast gain recovery and compression due to auger-assisted relaxation in quantum dot semiconductor optical amplifiers. Lightwave Technology Journalism, 2009, 27(13): 2530–2536
13. Kim J, Meuer C, Bimberg D, Eisenstein G. Effect of inhomogeneous broadening on gain and phase recovery of quantum-dot semiconductor optical amplifiers. IEEE Journal of Quantum Electronics, 2010, 46(11): 1670–1680
14. Xiao J L, Yang Y D, Huang Y Z. Investigation of gain recovery for InAs/GaAs quantum dot semiconductor optical amplifiers by rate equation simulation. Optical and Quantum Electronics, 2009, 41(8): 613–626
15. Bendelli G, Komori K, Arai S. Gain saturation and propagation characteristics of index-guided tapered-waveguide traveling-wave semiconductor laser amplifiers (TTW-SLAs). IEEE Journal of Quantum Electronics, 1992, 28(2): 447–458